

CrossMark
click for updatesCite this: *RSC Adv.*, 2016, 6, 88625

Reinforcement effects of nanocarbons on catalyst behaviour and polyethylene properties through *in situ* polymerization

M. Khoshsefat,^a S. Ahmadjo,^{*a} S. M. M. Mortazavi^a and G. H. Zohuri^b

MWCNT (multi-walled carbon nanotube), MWCNT-COOH and xGnP (exfoliated graphene nanoplatelet) were used in the *in situ* polymerization of ethylene in the presence of a binuclear complex (BNC₄) in which triisobutylaluminum (TiBA) and methylaluminoxane (MAO) were employed as cocatalysts. Functional groups on MWCNT-COOH, MWCNT and xGnP were masked with TiBA. In comparison to BNC₄ (503.3 g PE per mmol Ni per h), not only was the catalytic activity using BNC₄/xGnP (1811.8 g PE per mmol Ni per h) and BNC₄/MWCNT (1025.1 g PE per mmol Ni per h) improved, due to the adsorption of catalyst on the nanocarbon surface, but also the properties of the PE/nanocarbons were markedly affected. A DSC thermogram of PE/xGnP showed a peak together with a shoulder, which was broader than was observed with pure PE, whereas a narrow peak was observed for PE/MWCNT-COOH and for PE/MWCNT. Moreover, nanocarbons with a change in PE morphology were observed through SEM images. The unsaturation content and the extent of branching for polyethylene obtained using BNC₄/Nanocarbons were in the range of 7.6–16.8 and 186–214., respectively. The surface electrical conductivity improved substantially ($\approx 10^{-6}$ S cm⁻¹), relative to pure PE ($\approx 10^{-13}$ S cm⁻¹).

Received 23rd June 2016
Accepted 2nd September 2016

DOI: 10.1039/c6ra16243f

www.rsc.org/advances

Introduction

Nanomaterials (especially nanocarbons) have shown interesting effects on polymers, modifying or enhancing their properties.^{1,2} Nanocarbons can affect various properties of a polymer matrix, such as molecular weight, stiffness, toughness, electrical/thermal conductivity, thermal stability, and crystallinity.^{1–6} The nanocarbons can be incorporated into the polymer matrix through three main methods: synthesizing the nanocomposite by *in situ* polymerization,^{7–10} solution mixing^{11–13} and melt mixing.^{13–17} Among these, the *in situ* polymerization^{9,18} of olefins such as ethylene and propylene in the presence of nanocarbons is one of the most promising and efficient methods to synthesize polyolefin nanocomposites, or alternatively functional nanocarbons can be used as a co-monomer in polymer grafting.^{9,19–23} Also, the nanocarbons can act as a support or ligand for a coordinative polymerization catalyst.^{24–26} Overall, the synthesis of nanocarbon nanocomposites through *in situ* polymerization seems to be beneficial due to the fact that nanotube dispersion can be achieved in a solvent in which the monomer is also dissolved or suspended.²⁷

In a comparison between CNTs and graphene, CNTs have a lower surface to volume ratio due to the inaccessibility of the inner nanotube surface to polymer molecules.^{28–30} To fabricate graphene/polymer composites, several polymers have been used as a matrix.^{31–36} In addition, there is a good interfacial adhesion between the polyolefin matrix and carbon nanotubes. Many factors, including the type of nanocarbons used and their intrinsic properties, the dispersion state of nanocarbons in the polymer matrix and their interfacial interaction in the matrix, can affect the properties and application of nanocarbon/polymer composites. The hydrophobic surfaces of carbon nanotubes adsorb a wide variety of substances by van der Waals interactions.^{37,38} Graphene and carbon nanotubes are receiving a great deal of attention as an alternative matrix for catalyst and enzyme immobilization.

There are two approaches to immobilizing substances on the surface: covalent and noncovalent. Hydrophobic interactions of substances through their hydrophobic side chains with the surface of GnPs or the sidewall of CNTs can contribute to immobilization because of the highly hydrophobic nature of pristine nanocarbons. As for electrostatic interactions, the π -electrons on the surface of CNTs will interact with the π -electrons of aromatic rings.³⁸

According to the literature, catalytic polymerization using a nanocarbon/catalyst system, including nanocarbon/Ziegler-Natta,^{39–42} nanocarbon/metallocene^{8–10,25,26,43–47} and also nanocarbon/post-metallocene,^{10,19} has shown some beneficial

^aDepartment of Catalyst, Iran Polymer and Petrochemical Institute (IPPI), P.O. Box 14965/115, Tehran, Iran. E-mail: S.ahmadjo@ippi.ac.ir

^bDepartment of Chemistry, Faculty of Science, Ferdowsi University of Mashhad, P.O. Box: 91775, Mashhad, Iran

influence on catalyst performance, including maintaining or enhancing catalyst productivity, stability, and selectivity, and avoiding reactor fouling. There have also been beneficial effects on the properties of the produced polymer, such as mechanical, thermal and electrical conductivity, as a result of the incorporation of nanoparticles and nanotubes, with potential applications in the automotive, aerospace and electronics industries, etc.^{27,45,48}

In this paper, a synthesized binuclear catalyst was used. The aim of the research was to investigate the effect of nanocarbons on catalyst behaviour and on the properties of the resultant polyethylene. The polymerization of ethylene in the presence of a binuclear α -diimine Ni-based catalyst occurred directly on the nanocarbon surface. The effects of nanocarbons on catalyst performance and the resulting nanocomposite properties were significant.

Experimental

Materials

All manipulations of air- and/or water-sensitive compounds were conducted under an argon/nitrogen atmosphere using the standard Schlenk techniques. All the solvents were purified prior to use. Toluene (purity 99.9%) (Iran, Petrochemical Co.) was purified over sodium wire/benzophenone, and used as the polymerization solvent. Dichloromethane (purity 96%) (Sigma Aldrich Chemicals, Germany) was purified over calcium hydride powder and distilled prior to its use as a complex-synthesis solvent. Polymerization-grade ethylene gas (purity 99.9%) (Iran, Petrochemical Co.) was purified by passing it through activated silica gel, KOH, and a 4 Å/13× molecular sieve column. 2,6-Diisopropyl aniline, 1,4-phenylene diamine, acenaphthoquinone, nickel(II) bromide ethylene glycol dimethyl ether complex [(DME)·NiBr₂] (purity 97%) and diethyl ether (purity 99.5%) were supplied by Merck Chemicals (Darmstadt, Germany) and used in the synthesis of ligands and catalysts. Triisobutylaluminium (purity 93%) (TiBA), supplied by Sigma Aldrich Chemicals (Steinheim, Germany), was used as cocatalyst, masking agent and reactant in the synthesis of MAO according to the literature.⁴⁹ MWCNT (>50 nm) and MWCNT-COOH (8–15 nm) were purchased from Neunano (Tehran, Iran) and GnPs (grade M) were supplied by XG Sciences (East Lansing, USA).

Characterization

FT-IR spectra were obtained using a Thermo Nicolet AVATAR 370 instrument. Differential scanning calorimetry (DSC) (Mettler Toledo DSC822) and thermal gravimetric analysis (TGA) (Perkin Elmer TGA-7) with a rate of 10 °C min⁻¹ were used for characterization of polymer and nanocomposites. The morphologies of the polymer and nanocomposites were studied by a scanning electron microscopy (SEM) (LEO 1450VP) technique. Electrical resistance was performed with resistance thermometers from the Rizpardazan Company of Iran, 4PP-R2K model, according to ASTM D257 and F-84 standards.

Preparation of complex BNC₄

The ligand and corresponding catalyst BNC₄ were synthesized according to our previously reported work.⁵⁰

Polymerization procedure

Ethylene polymerization was carried out in a reactor which was equipped with a Schlenk system, vacuum line, ethylene inlet (Buchi bmd 300 type reactor) and magnetic stirrer.

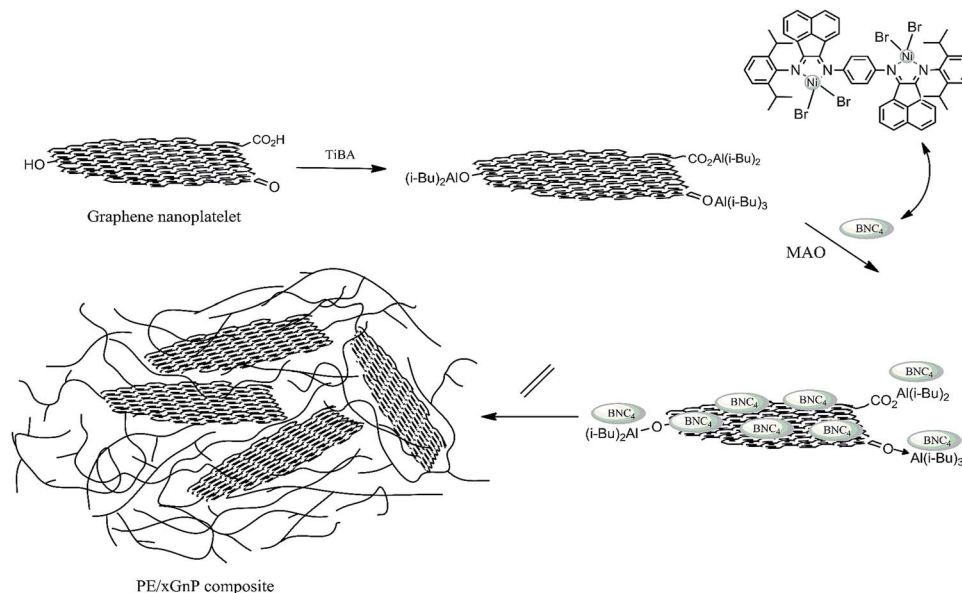
Results and discussion

In situ polymerization

In order to compare the effect of nanocarbons on the catalyst behaviour and properties of the produced nanocomposite, the ethylene polymerization was carried out in the presence of BNC₄ and BNC₄/nanocarbon systems, and MAO and TiBA were also used as co-catalysts. A modified procedure was employed to anchor the catalyst on the nanocarbon surface.^{10,25,43} The key to the synthesis of the nanocomposites is a good dispersion of nanoparticles. To achieve this goal, the mixture was completely stirred for about 20 minutes prior to and after injection into the reactor, in order to obtain a good dispersion throughout the *in situ* polymerization. In this method, a mixture of the nanocarbon and triisobutylaluminium (TiBA) was stirred to mask the functional groups (naturally occurring functional groups such as ethers, carboxyls, or hydroxyls, according to factory MSDS and FT-IR analysis) at the edges of the graphene platelets, and carboxyl groups in MWCNT-COOH. In this state, TiBA can act as an impurities scavenger. As depicted in Scheme 1, after reaction with TiBA, xGnP and BNC₄/MAO, the catalyst can be immobilized and be partially active with alkyl aluminium.^{51,52} The reactions of alkyl aluminium compounds and hydroxyl, carboxyl and amine groups are completely described in the literature references.^{53,54} There are proposed mechanisms for this type of immobilization, including π - π stacking of aromatic rings and electrostatic interaction of alkyl aluminium and active species.^{27,51,53,55,56}

In this paper, the authors considered both of these mechanisms, due to the presence of the phenyl and acenaphthenyl aromatic rings in the ligand structure of the BNC₄ that improve the π - π interaction and immobilization of the catalyst. In addition, the electrostatic interaction between the positive active species and the negative masked species at the edge of the nanocarbons should also be considered. However, according to the results for BNC₄/xGnP, the π - π stacking is stronger and more effective. The principal reaction for activation of the catalyst is shown in Fig. 1.⁵⁶ The presence of nanocarbons through the use of this method can make the system into a semi-heterogeneous system which can be active with common alkyl aluminium compounds such as TiBA.

The amount of nanocarbons was equal (1 : 1) (w/w) to the amount of BNC₄. After polymerization, the nanocomposite produced was precipitated using 5% v/v acidic methanol. According to Fig. 2, the catalytic performances using MAO as cocatalyst were higher than with TiBA for BNC₄, BNC₄/



Scheme 1 Procedure for immobilizing the catalyst on the xGnP.

MWCNT and BNC₄/xGnP; however, MAO was less effective for the BNC₄/MWCNT-COOH catalytic system. This can be ascribed to the nature of the cocatalyst and nanocarbon and the interaction between them.¹⁹ Moreover, TiBA could act as an activator in the BNC₄/nanocarbon system but less effectively than MAO. This behaviour has been used to assign the

best combination according to the alkylating ability and acidity of the MAO.⁵⁷

In some reports, using a catalyst/nanocarbon system in olefin polymerization showed an increase in activity, branching degree, broadening PDI and decreasing crystallinity and melting point.^{10,19,25,40,43} In this work, based on the yield of nanocomposites, xGnP and MWCNT exhibited a remarkable and striking influence on catalyst behaviour due to the direct adsorption of catalyst onto the surface of the nanocarbons. The nonfunctional surface leads to physisorption arising from attractive interaction (van der Waals forces). In comparison with nanocarbons, graphene has a higher surface to volume ratio.

Based on this, anchoring the catalyst on nanocarbons and distributing active centres is better than using CNTs. In

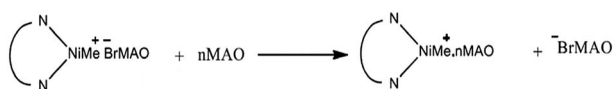


Fig. 1 Mechanism of catalyst activation in the presence of the MAO.

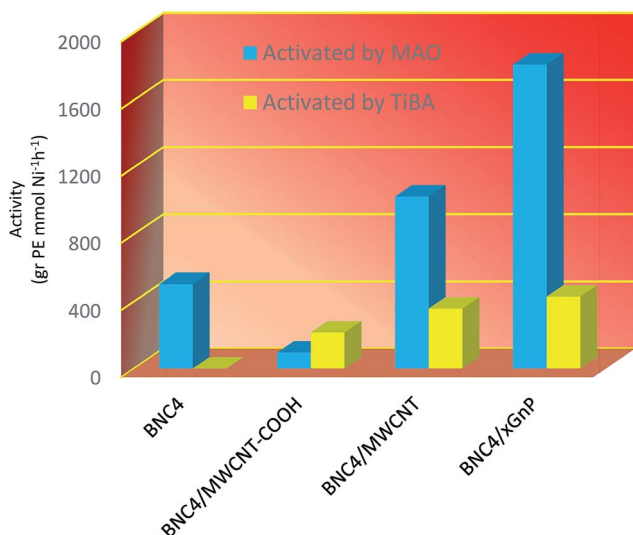


Fig. 2 Polymerization of ethylene using the BNC₄/nanocarbon system activated by MAO and TiBA.

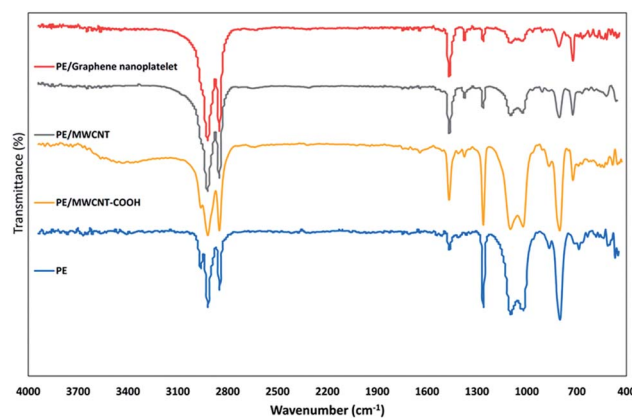
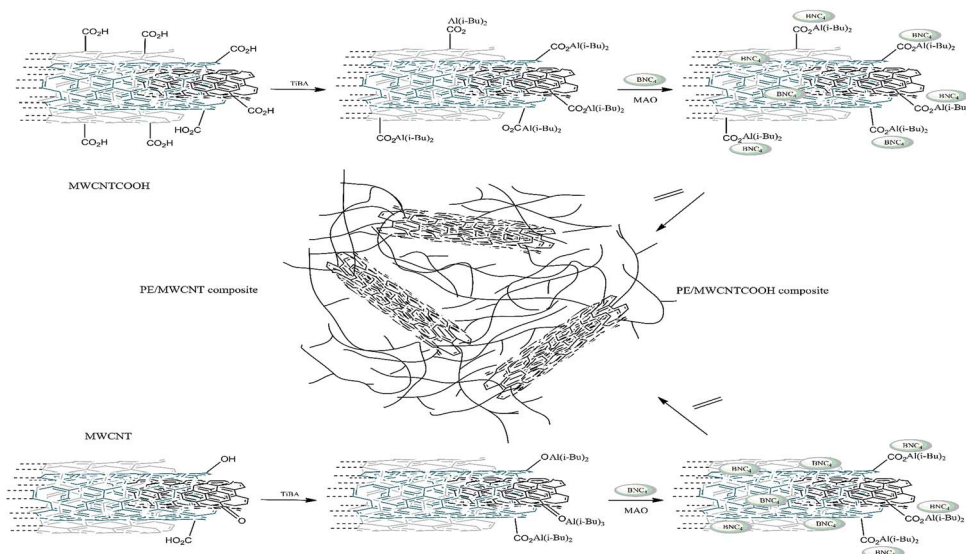


Fig. 3 FT-IR spectra of the PE and PE/nanocarbon nanocomposites.



Scheme 2 Procedure for immobilizing the catalyst on the MWCNT.

Table 1 Ethylene polymerization using BNC₄ and BNC₄/nanocarbon catalytic system

Entry	Catalytic system	Cocatalyst	Crystallinity%	C=C (in 1000 C)	Branching (in 1000 C)
1 ^a	BNC ₄	MAO	24.3	9.4	78
2	BNC ₄	TiBA	n.d.	n.d.	n.d.
3	BNC ₄ /MWCNT-COOH	MAO	2.8	16.8	237
4	BNC ₄ /MWCNT-COOH	TiBA	1.1	17.2	246
5	BNC ₄ /MWCNT	MAO	7.9	11.0	198
6	BNC ₄ /MWCNT	TiBA	2.3	14.3	201
7	BNC ₄ /xGnP	MAO	16.2	7.6	224
8	BNC ₄ /xGnP	TiBA	4.5	3.3	153

^a Extracted from ref. 48, polymerization conditions: (catalyst : nanocarbon) = (% w/w) = 1, [Al]/[Ni] = 2000, monomer pressure 1.5 bar, polymerization time 1 h, polymerization temperature 26 °C, [BNC₄] = 4.2 × 10⁻³ mmol.

contrast, using the BNC₄/MWCNT-COOH catalyst system indicated a significant adverse effect on catalyst activity when it was treated with TiBA. An FT-IR spectrum of the polyethylene obtained by this catalytic system (Fig. 3) showed the presence of carboxylic acid groups in the product (C=O at 1647 cm⁻¹ and a broad peak at range 3200–400 cm⁻¹). This is due to carboxyl groups which could cause deactivation of the catalytic centres (Scheme 2).

The infrared spectra (Fig. 3) of samples in the region of 1360–1380 cm⁻¹ and 720–730 cm⁻¹ arise from the symmetrical deformation of methyl groups and from the rocking of methylene groups perpendicular to the chain direction (crystalline regions), respectively.⁵⁷

Consideration of the intensities at 723 cm⁻¹ and 1370 cm⁻¹ of the samples provides evidence of the decreasing crystallinity from polyethylene to PE/nanocarbon composite, as calculated using DSC data (Table 1). Also, the aliphatic vinyl content and branching degree of samples were determined according to our recent work.⁴⁸

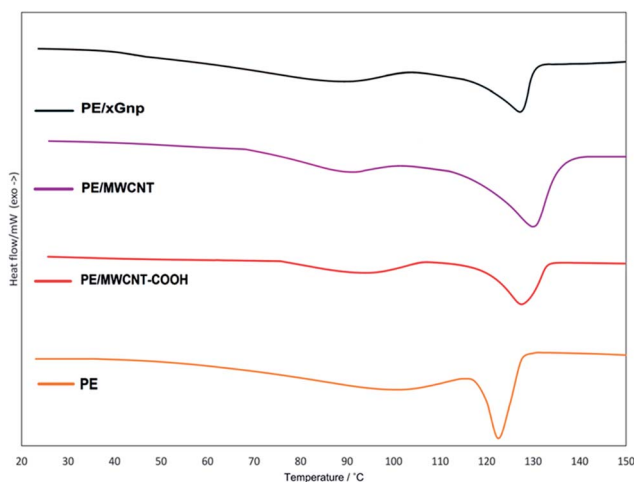


Fig. 4 DSC thermograms of the PE and PE/nanocarbon composites synthesized through *in situ* polymerization using the BNC₄/MAO system.

For all nanocomposites, the vinyl content was higher than for pure PE, exceptionally so for PE/xGnP. The highest amount belonged to PE/MWCNT-COOH which was attributed to the electronic effect of the presence of electronegative groups which can increase the β -hydrogen elimination reaction. The branching degrees of the PE/nanocarbon composites were all higher than for pure PE.

In the DSC study (Fig. 4), a similar broadening transition in melting was observed in all samples, which has been attributed to a sequence of melting followed by recrystallization steps of less ordered domains with variable degrees of chain branching.⁴⁸ By considering the increase in branching degree in the nanocomposites, the decrease in the extent of crystallinity is visible. The main melting point shifted to a greater extent for PE/nanocarbon composites in comparison to PE. Nanocarbons play a constraining role in the mechanism of PE chain growth, by interaction with the catalyst and/or the active centre of propagation.⁵⁸ We ascribed all of these observations relating to microstructure and thermal properties to the presence of nanocarbons. Although they can act as a support for the catalyst and distribute the active centres, facilitating monomer accessibility and enhancing catalytic performance, they can also make it possible to increase β -hydrogen elimination and chain transfer reactions to the monomer or catalyst and dissociation of the linked polymer chain from the metal center.⁹

Thermogravimetric curves resulting from thermal gravimetric analysis (TGA) (Fig. 5) did not show any significant change in degradation, but the onset of degradation temperature for PE (240 °C) increased in the presence of MWCNT (245 °C) and MWCNT-COOH (250 °C), though it was diminished for the graphene nanocomposite (225 °C).⁴¹ Differential thermogravimetric curves (Fig. 6) clarified that sample degradation occurred mainly in the range 400–500 °C. There is also a peak for PE/MWCNT-COOH at a higher temperature

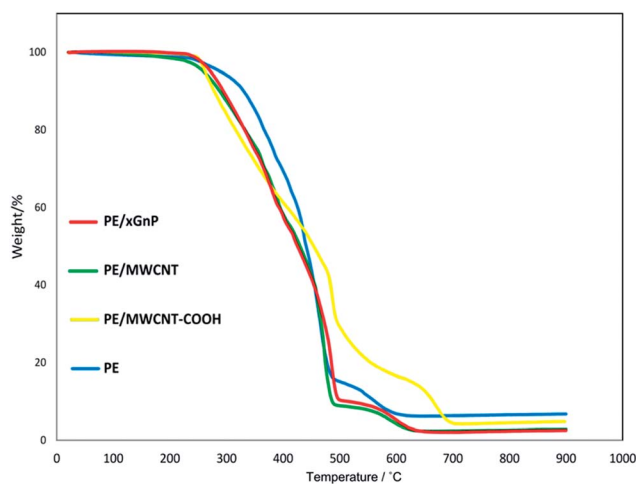


Fig. 5 Thermogravimetric curves of the PE and PE/nanocarbon composites synthesized through *in situ* polymerization in the presence of the BNC₄/MAO system.

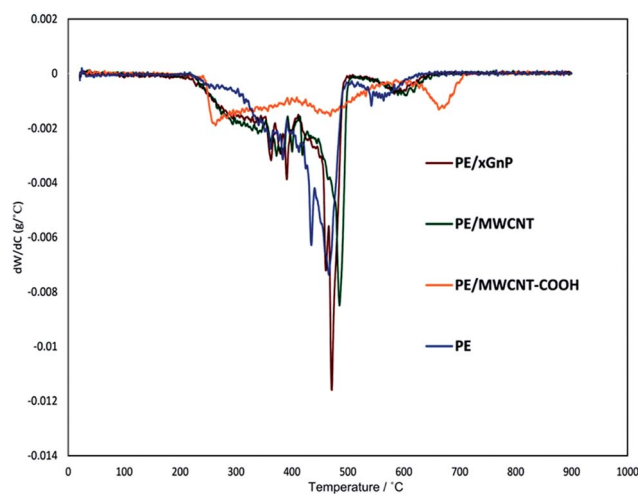


Fig. 6 Differential thermogravimetric curves of the PE and PE/nanocarbon composites synthesized through *in situ* polymerization in the presence of the BNC₄/MAO system.

Table 2 Specific conductivity of PE/nanocarbons

Entry	Sample	Specific electric conductivity (S cm ⁻¹)
1	PE	10 ⁻¹³
2	PE/MWCNT-COOH	2.37 × 10 ⁻⁶
3	PE/MWCNT	1.54 × 10 ⁻⁶
4	PE/xGnP	1.07 × 10 ⁻⁸

(660 °C). This observation was attributed to the higher thermal stability of MWCNT-COOH, which can be observed in the nanocomposite.

In many articles, it has been noted that polymer nanocomposites have shown better electrical and thermal conductivity because of the nature of the nanocarbon's conductivity, which can be imparted to the polymer.^{4,27,59} Accordingly, the electrical conductivities of the pure PE and PE/nanocarbons were measured and compared. The electrical conductivity of the PE/MWCNT-COOH composite was the highest and altogether PE/nanocarbons showed a significant effect on the electrical conductivity (Table 2).

The morphologies of the resulting samples through *in situ* synthesis of polyethylene nanocomposite and placement of the nanocarbons in the polymer matrix were studied by SEM images. As depicted in Fig. 7, there is a soft and flower-like shape in (a–c) of PE.⁹ The morphology of PE/xGnP (d–f) showed a change in morphology, with a soft and uniform surface. It was rubber-like in appearance. Images of PE/MWCNT-COOH and PE/MWCNT are presented in Fig. 7g–i and j–l, respectively. The presence of nanotubes is obvious, in which CNTs acted as a bridge and end-cap in the polymer matrix.²⁵

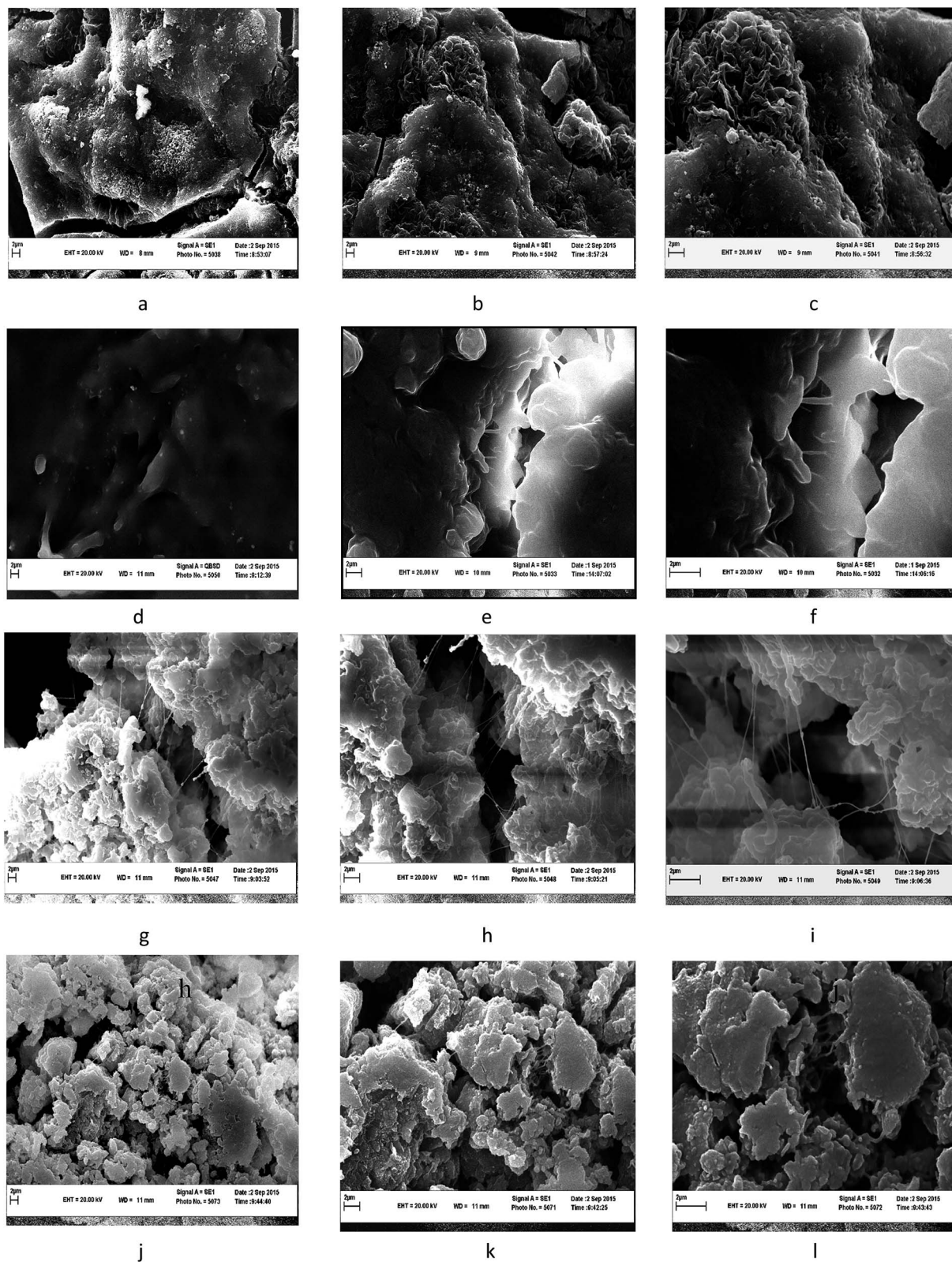


Fig. 7 SEM images of (a–c) PE (d–f) PE/xGnP (g–i) PE/MWCNT (j–l) PE/MWCNT-COOH.

Conclusions

The synthesis of polyethylene/nanocarbon composites through *in situ* polymerization was advantageous, producing a good

dispersion of nanocarbons within the polymer matrix. In addition, this type of synthesis showed a beneficial influence on several aspects of performance, enhancing catalyst activity, avoiding reactor fouling and improving the properties of the

produced polymer. In this report, a binuclear late transition metal catalyst was used in the presence of MAO and TiBA as activators. Functional groups on MWCNT-COOH, MWCNT and xGnP were masked with TiBA. This treatment was effective for xGnP and MWCNT, but not for MWCNT-COOH. Pre-mixing of the nanocarbons and BNC₄ led to the adsorption of the catalyst onto the nanocarbon surface, involving both hydrophobic and electrostatic interactions. Although MWCNT-COOH with functional groups can cause deactivation of catalyst active centres even with TiBA treatment, noncovalent immobilization of the catalyst on the hydrophobic surface of the nanocarbons nevertheless produced a striking improvement in catalyst behaviour. Moreover, the thermal and microstructural properties of the polyethylene, such as crystallinity extent, melting point, vinyl content and branching degree, were strongly affected by the presence of nanocarbons in the catalyst system and polymer matrix. Nanocarbons impart their remarkable electrical properties to the resulting polyethylene product.

Acknowledgements

The authors are thankful of Iran Polymer and petrochemical Institute (IPPI) and Ferdowsi university of Mashhad (FUM) for all their cooperation.

Notes and references

- M. S. Dresselhaus, G. Dresselhaus and P. Avouris, *Carbon Nanotubes: Synthesis, Structure, Properties, and Applications*, Springer-Verlag, Berlin Heidelberg, 2001, ch. 1 and 14, vol. 80, pp. 1–9, 391–425.
- Y. Boyjoo, K. Merigot, J. F. Lamonier, V. K. Pareek, M. O. Tade and J. Liu, *RSC Adv.*, 2015, **5**, 24872–24876.
- H. Kim, A. A. Abdala and C. W. Macosko, *Macromolecules*, 2010, **43**, 6515–6530.
- J. R. Potts, D. R. Dreyer, C. W. Bielawski and R. S. Ruoff, *Polymer*, 2011, **52**, 5–25.
- V. Mittal, G. E. Luckachan and N. B. Matsko, *Macromol. Chem. Phys.*, 2014, **215**, 255–268.
- J. Liu, N. P. Wickramaratne, S. Z. Qiao and M. Jaroniec, *Nat. Mater.*, 2015, **14**, 763–774.
- H. Kong, C. Gao and D. Yan, *J. Am. Chem. Soc.*, 2004, **126**, 412–413.
- A. Funck and W. Kaminsky, *Compos. Sci. Technol.*, 2007, **67**, 906–915.
- L. Boggioni, G. Scalcione, A. Ravasio, F. Bertini, C. D. Arrigo and I. Tritto, *Macromol. Chem. Phys.*, 2012, **213**, 627–634.
- L. Zhang, E. Yue, B. Liu, P. Serp, C. Redshaw, W. H. Sun and J. Durand, *Catal. Commun.*, 2014, **43**, 227–230.
- O. Breuer and U. Sundararaj, *Polym. Compos.*, 2004, **25**, 630–645.
- J. Suhr, W. Zhang, P. M. Ajayan and N. A. Koratkar, *Nano Lett.*, 2006, **6**, 219–223.
- Y. Y. Huang and E. M. Terentjev, *Polymers*, 2012, **4**, 275–295.
- Y. F. Shih, L. S. Chen and R. J. Jeng, *Polymer*, 2008, **49**, 4602–4611.
- L. F. Giraldo, B. L. Lopez and W. Brostow, *Polym. Eng. Sci.*, 2009, **49**, 896–902.
- B. Lin, U. Sundararaj and P. Potschke, *Macromol. Mater. Eng.*, 2006, **291**, 227–238.
- J. Y. Kim, D. K. Kim and S. H. Kim, *Eur. Polym. J.*, 2009, **45**, 316–324.
- V. Mittal, *Polymer Nanotubes Nanocomposites: Synthesis, Properties and Applications*, John Wiley & Sons, 2014, ch. 1, pp. 4–18.
- L. Zhang, E. Castillejos, P. Serp, W. H. Sun and J. Durand, *Catal. Today*, 2014, **235**, 33–40.
- D. E. Hill, Y. Lin, A. M. Rao, L. F. Allard and Y. P. Sun, *Macromolecules*, 2002, **35**, 9466–9471.
- W. Guojian, Q. Zehua, L. Lin, S. Quan and G. Jianlong, *Mater. Sci. Eng., A*, 2008, **472**, 136–139.
- D. Baskaran, J. W. Mays and M. S. Bratcher, *Polymer*, 2005, **46**, 5050–5057.
- Y. Lin, B. Zhou, K. A. S. Fernando, P. Liu, L. F. Allard and Y. P. Sun, *Macromolecules*, 2003, **36**, 7199–7204.
- B. Zhao, H. Hu, A. Yu, D. Perea and R. C. Haddon, *J. Am. Chem. Soc.*, 2005, **127**, 8197–8203.
- X. Dong, L. Wang, L. Deng, J. Li and J. Huo, *Mater. Lett.*, 2007, **61**, 3111–3115.
- S. Park, H. J. Paik, S. W. Yoon, I. S. Choi, K. B. Lee, D. J. Kim, Y. H. Jung and Y. Do, *Macromol. Rapid Commun.*, 2006, **27**, 47–50.
- W. Kaminsky, *Polymer–Carbon Nanotube Composites*, Woodhead Publishing, 2011, pp. 3–24.
- S. Stankovich, D. A. Dikin, G. H. B. Dommett, K. M. Kohlhaas, E. J. Zimney, E. A. Stach, R. D. Piner, S. T. Nguyen and R. S. Ruoff, *Nature*, 2006, **442**, 282–286.
- J. N. Coleman, U. Khan, W. J. Blau and Y. K. Gunko, *Carbon*, 2006, **44**, 1624–1652.
- O. Breuer and U. Sundararaj, *Polym. Compos.*, 2004, **25**, 630–645.
- S. L. Qiu, C. S. Wang, Y. T. Wang, C. G. Liu, X. Y. Chen, H. F. Xie, Y. A. Huang and R. S. Cheng, *EXPRESS Polym. Lett.*, 2011, **5**, 809–818.
- X. Zhao, Q. Zhang, D. Chen and P. Lu, *Macromolecules*, 2010, **43**, 2357–2363.
- M. Yoonessi and J. R. Gaier, *ACS Nano*, 2010, **4**, 7211–7220.
- Y. S. Yun, Y. H. Bae, D. H. Kim, J. Y. Lee, I.-J. Chin and H.-J. Jin, *Carbon*, 2011, **49**, 3553–3559.
- P. Song, Z. Cao, Y. Cai, L. Zhao, Z. Fang and S. Fu, *Polymer*, 2011, **52**, 4001–4010.
- H. Kim, S. Kobayashi and M. A. AbdurRahim, *Macromol. Chem. Phys.*, 2012, **213**, 1060–1077.
- S. Banerjee, T. Hemraj-Benny and S. S. Wong, *Adv. Mater.*, 2005, **17**, 17–29.
- N. Saifuddin, A. Z. Raziah and A. R. Juniza, *J. Chem.*, 2013, DOI: 10.1155/2013/676815.
- X. Tong, C. Liu, H. M. Cheng, H. Zhao, F. Yang and X. Zhang, *J. Appl. Polym. Sci.*, 2004, **92**, 3697–3700.
- Z. Liu, M. Yu, J. Wang, F. Li, L. Cheng, J. Guo, Q. Huang, Y. Zhou, B. Zhu, J. Yi, Y. Liu and W. Yang, *J. Ind. Eng. Chem.*, 2013, **20**, 1804–1811.

- 41 J. Steinmetz, H. J. Lee, S. Kwon, D. S. Lee, C. Goze-Bac, E. Abou-Hamad, H. Kim and Y. W. Park, *Curr. Appl. Phys.*, 2007, **7**, 39–41.
- 42 N. Wang, Y. Qin, Y. Huang, H. Niu, J. Y. Dong and Y. Wang, *Appl. Catal., A*, 2012, **435**, 107–114.
- 43 D. Bonduel, M. Mainil, M. Alexandre, F. Monteverde and P. Dubois, *Chem. Commun.*, 2005, 781–783.
- 44 S. Li, W. Cheng, H. Chen, M. Li, W. Bi, L. Li, J. Zhou and T. Tang, *J. Polym. Sci., Part A: Polym. Chem.*, 2007, **45**, 5459–5469.
- 45 M. A. Milani, D. González, R. Quijada, N. R. S. Basso, M. L. Cerrada, D. S. Azambuja and G. B. Galland, *Compos. Sci. Technol.*, 2013, **84**, 1–7.
- 46 W. Kaminsky, A. Funck and K. Wiemann, *Macromol. Symp.*, 2006, **239**, 1–6.
- 47 W. Kaminsky, A. Funck and C. Klinke, *Top. Catal.*, 2008, **48**, 84–90.
- 48 H. Tian, M. Saunders, A. Dodd, K. O'Donnell, M. Jaroniec, S. Liu and J. Liu, *J. Mater. Chem. A*, 2016, **10**, 3721–3727.
- 49 S. A. Sangokoya, Preparation of aluminoxanes, EP 0463555 B1, 1996.
- 50 M. Khoshsefat, G. H. Zohuri, N. Ramezani, S. Ahmadjo and M. Haghpanah, *J. Polym. Sci., Part A: Polym. Chem.*, 2016, **18**, 3000–3011.
- 51 H. S. Cho and W. Y. Lee, *Korean J. Chem. Eng.*, 2002, **19**, 557–563.
- 52 E. Y. X. Chen and T. J. Marks, *Chem. Rev.*, 2000, **100**, 1391–1434.
- 53 S. Pasykiewicz, *Pure Appl. Chem.*, 2009, **30**(3–4), 509–522.
- 54 J. J. McKetta, *Encyclopedia of Chemical Processing and Design*, Marcel Dekker, New York, 2002, ch. 1, vol. 3, pp. 1–57.
- 55 S. Banerjee, J. H. Lee, T. Kuila and N. H. Kim, Synthesis of graphene-based polymeric nanocomposites, in *Fillers and Reinforcements for Advanced Nanocomposites*, Woodhead Publishing, 2015, ch. 7, pp. 133–155.
- 56 S. Damavandi, N. Samadieh, S. Ahmadjo, Z. Etemadina and G. H. Zohuri, *Eur. Polym. J.*, 2015, **64**, 118–125.
- 57 C. G. deSouza, R. F. de Souza and K. Bernardo-Gusmao, *Appl. Catal., A*, 2007, **325**, 87–90.
- 58 P. Fabbri, E. Bassoli, S. B. Bon and L. Valentini, *Polymer*, 2012, **53**, 897–902.
- 59 J. Du and H. M. Cheng, *Macromol. Chem. Phys.*, 2012, **213**, 1060–1077.